

## Article

# Polypropylene Composites Reinforced with Lignocellulose Nanocrystals of Corncob: Thermal and Mechanical Properties

Edgar Mauricio Santos-Ventura <sup>1</sup>, Marcos Alfredo Escalante-Álvarez <sup>2</sup>, Rubén González-Nuñez <sup>3</sup> ,  
Marianelly Esquivel-Alfaro <sup>4</sup> and Belkis Sulbarán-Rangel <sup>1,\*</sup> 

<sup>1</sup> Department of Water and Energy, Campus Tonalá, University of Guadalajara, Tonalá 45425, Mexico; mauricio.santos@academicos.udg.mx

<sup>2</sup> Department of Wood Pulp and Paper, CUCEI, University of Guadalajara, Guadalajara 45020, Mexico; marcos.escalante@academicos.udg.mx

<sup>3</sup> Department of Chemical Engineering, CUCEI, University of Guadalajara, Guadalajara 44430, Mexico; ruben.gnunez@academicos.udg.mx

<sup>4</sup> Laboratory of Polymer Science and Technology (POLIUNA), School of Chemistry, Campus Omar Dengo, Universidad Nacional de Costa Rica, Heredia 40101, Costa Rica; mesquive@una.ac.cr

\* Correspondence: belkis.sulbaran@academicos.udg.mx

**Abstract:** Composites based on recycled polypropylene (PP) reinforced with cellulose nanocrystals whit lignin corncob were prepared. The effect of the ratio composites prepared via a compression molding process on the mechanical and thermal properties was analyzed. Corncobs is a little-used agroindustrial residue with a high cellulose content. The corncob was milled and then delignified via the organosolve process in order to get the cellulose unbleached. An acid hydrolysis process was then carried out to obtain lignocellulose nanocrystals (LCNCs). Subsequently, LCNC/PP composites were obtained via termocompression molding using different concentrations of LCNC (0, 0.5, 1 and 2% by weight) previously mixed via extrusion. The residual lignin present in the LCNCs improved the compatibility between the reinforcement and the PP matrix. This was evidenced by the increase in mechanical properties and the stabilization of thermal properties. The results of the mechanical tests showed that the LCNC increases the tensile and flexural modules and strength with respect to neat PP. Composites with 2% of LCNC showed an increase of 36% and 43% in modulus and tensile strength, respectively, while the flexural modulus and strength increased by 7.6%. By using reinforcements of natural and residual origin (corncob) and improving the properties of recycled polymers, their reuse will increase, and this can lead to reducing waste in the environment.

**Keywords:** composites; residual lignin; compression molding; mechanical properties; thermal properties



**Citation:** Santos-Ventura, E.M.; Escalante-Álvarez, M.A.; González-Nuñez, R.; Esquivel-Alfaro, M.; Sulbarán-Rangel, B. Polypropylene Composites Reinforced with Lignocellulose Nanocrystals of Corncob: Thermal and Mechanical Properties. *J. Compos. Sci.* **2024**, *8*, 125. <https://doi.org/10.3390/jcs8040125>

Academic Editor: Francesco Tornabene

Received: 26 February 2024

Revised: 10 March 2024

Accepted: 19 March 2024

Published: 29 March 2024



**Copyright:** © 2024 by the authors. Licensee MDPI, Basel, Switzerland. This article is an open access article distributed under the terms and conditions of the Creative Commons Attribution (CC BY) license (<https://creativecommons.org/licenses/by/4.0/>).

## 1. Introduction

Composite materials are one of the fastest growing sectors and a marvel of modern science [1]. Most composite materials have been created to improve and combine mechanical properties such as stiffness, toughness and tensile strength at room temperature and at elevated temperatures. Most composite materials are made up of two phases; one called the matrix, which is continuous and surrounds the other phase, which is called the dispersed phase or reinforcement [2]. The use of a matrix and a reinforcement will depend on the final use that will be given to the composite material. Recently, there has been a great boom in using fibers of natural origin as reinforcements in various polymeric matrices since these fibers have important characteristics of resistance and biodegradability that make them more environmentally friendly when the composite material is discarded [3–6]. This is important to consider since, worldwide, there is a great problem of the poor disposal of plastic waste of synthetic origin derived from petroleum.

Today, many synthetic polymers are used as a matrix and reinforced with fibers to make composite materials. A widely used polymer is polypropylene (PP) [6–8]. This is

a thermoplastic material whose production and applications have a significant growth worldwide, only surpassed by polyethylene (PE) and polyvinyl chloride (PVC), which, due to its chemical structure, is easily recyclable [9]. In the automotive industry, the passenger cabin of automobiles uses PP to manufacture about 55% of the components, including the instrument panel, door panel, glove box, air conditioning and many others [10]. Despite the wide use of PP, research is constantly being carried out to improve its properties. Some examples of studies carried out on PP are those carried out with natural fibers such as milkweeds, sisals, agaves, olive pits, rice husks, jutes, and kenaf, among others [5,6]. In addition to this, PP has been reinforced with natural fibers on a nanometric scale such as cellulose nanocrystals (CNCs) [11,12]. The production of polymer mixtures with CNC to obtain nanocomposites has received increasing interest in recent years [7,8]. This is because the mixtures of its components promise to have better mechanical characteristics than each component separately, in addition to the fact that the CNC reinforcements have low density, are biodegradable and are from renewable sources [13,14].

However, since PP is a non-polar matrix and CNCs are polar, there is a need to improve compatibility between both. To improve the compatibility between the PP matrix and the CNC filler, it has been decided to carry out chemical modifications on the surface of the CNC and PP to improve dispersibility in the matrix and compatibility. Some research has reported the use of toluene diisocyanate [15], PP grafted with maleic anhydride [13,14], acetylated CNCs [16] and poly(ethylene-co-vinyl alcohol) [17]. It was shown that high-temperature processing has a significant effect on rheological behavior and mechanical properties. Recent research mentions reinforcing PP with basalt fiber (BF) and CNC to improve the resistance of the composite material due to the synergistic effect between the two reinforcements. The author mention that the CNCs not only promoted the crystallinity of PP through heterogeneous nucleation but also formed a wedge-shaped structure between themselves and the BFs through hydrogen bonds to prevent the molecular movement of PP. On the other hand, BFs promoted not only the extrusion crystallization of the resin matrix, but also the network structure formed by the appropriate BF content can realize the rapid external strength transmission [7]. In addition to this, there are difficulties due to agglomeration when adding nanoparticles to thermoplastic polymers such as PP. Studies have been reported with other nanoparticles, for example, carbon nanotubes, aluminas and others [18–20], where they mention accepted methods for mixing them and reducing the challenges of mixing and overcoming agglomeration. In studies carried out with CNC, it is recommended to use quantities less than 3% to avoid exhaustion problems [13,21,22].

With all this background, it is a fact that for a PP and CNC composite material to have good mechanical properties, it is necessary to make chemical modifications to the CNCs, such as adding another reinforcement or a coupling agent. Therefore, in this research, it is proposed to prepare fiber CNCs of unbleached corncob cellulose. When preparing CNC with unbleached cellulose, the residual lignin that remains after the cellulose isolation process is used [23]. Lignin is a very complex branched phenolic polymer, formed by heterogeneous units and is also the cementing material that binds cellulose fibers. It has been shown that with unbleached cellulose and applying acid hydrolysis, it is possible to have residual lignin in nanocrystals [23,24]. It has been reported that the chemical compatibility and physical and mechanical properties of PP films can be improved with nanofibers with residual lignin [25] and with CNC with residual Kenaf lignin [23]. Therefore, the novelty of this research is to prepare a recycled PP composite material with different concentrations of CNC with residual lignin (LCNC) from corncob. For this, the mixture was carried out by an extruder and then the composite material was produced in pellet form and, via this thermocompression, was made the final material for evaluations of its mechanical and thermal properties. Corncob is a residual biomass that is generated after shelling corn and is a rarely used raw material but with great potential to extract CNC [24]. The motivation to carry out this type of research was to improve the properties of a recycled polymer such as PP, and a residual biomass such as corncob was used to obtain an advanced material such as LCNC as reinforcement. The PP/LCNC composite material obtained better mechanical

property values than the single matrix of PP. The development of high-performance composite materials from residual biomass and polymer recycling are increasing worldwide and has attracted much attention due to economic and environmental concerns of the useful life of synthetic polymers [6,14].

## 2. Materials and Methods

### 2.1. Materials

Corncob from the Nextipac area, Municipality of Zapopan, Jalisco, Mexico, was used as agroindustrial residue. The corncob was crushed and sieved into a 40–60 mesh. The reagents used were the following:  $H_2SO_4$  (97%), undenatured  $CH_3CH_2OH$  (96%) and  $CH_3COOH$  (99.7%), and all of them were purchased from Sigma-Aldrich (Toluca, Mexico). The recycled polypropylene was white and in the form of granules ( $30 \times 10$  mm), and it was obtained from the company Plasticruz C.A. Tonalá, Jalisco, Mexico. According to the technical sheet, the characteristics of recycling PP were a melting flow rate ( $230^\circ C/2.16$  kg) of 17 g/10 min [26], a melting temperature of  $160\text{--}180^\circ C$  and density of  $0.9\text{ g/cm}^3$  [27]. Figure 1 shows the different manufacturing steps of the PP/LCNC composite material of this research.

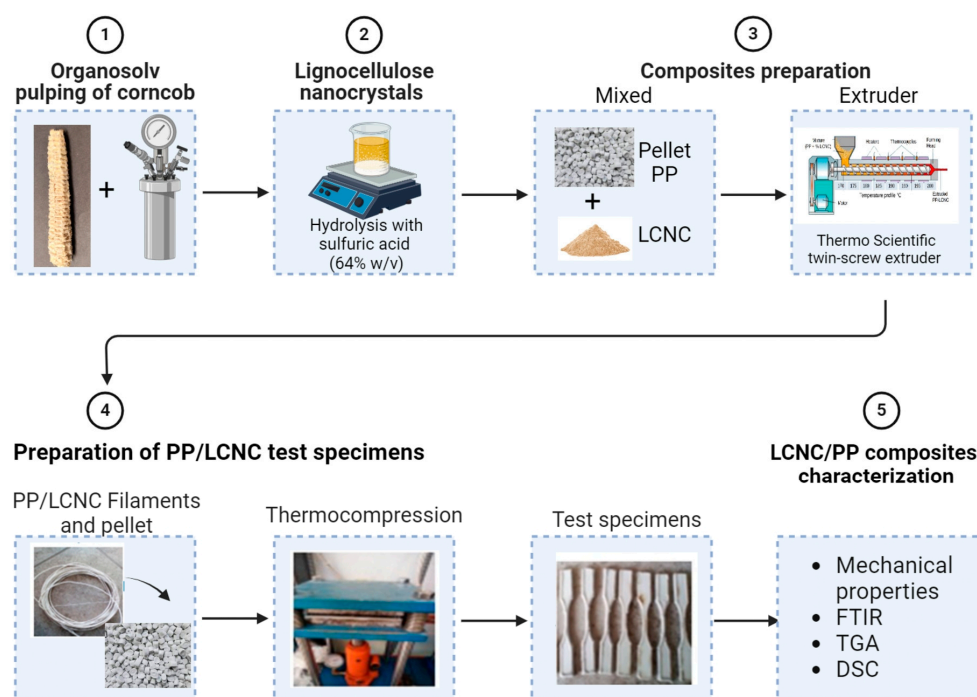


**Figure 1.** General experiment diagram.

### 2.2. Organosolv Pulping of Corncob

In a Jaime high-pressure digester, 400 g (dry weight) of corncob was added, with a 50% ethanol solution plus 12 milliliters of acetic acid. A 1:10 hydromodulus was used, in accordance with previous work [28,29]. With this treatment, cellulose with lignin residues was obtained. No bleaching was carried out since the idea was to have the cellulose functionalized with the lignin groups. The corncob and cellulose fiber were characterized via a scanning electron microscope (SEM) (TESCAN, model MIRA 3 LMU, Brno, Czechia). The images obtained were analyzed with the software ImageJ 1.45 to determine the fiber length and diameter.

### 2.3. Lignocellulose Nanocrystals

The unbleached cellulose obtained in the organosolv process was treated via acid hydrolysis with sulfuric acid ( $64\% w/v$ ) in a proportion of 1:10 at  $45^\circ C$  for 30 min with stirring

of the mixture according to the methodology previously reported by other authors [30]. The suspension was centrifuged at 6000 rpm for 15 min to remove excess acid. The resulting precipitate was dialyzed for 5 days, and tubular membranes (MWCO 3.5 kDa) were used until a neutral pH was reached. Subsequently, it was subjected to 20 min of ultrasound in an ice water bath. The lignocellulose nanocrystals (LCNCs) obtained in suspension were lyophilized to eliminate moisture and facilitate mixing with polypropylene. LCNC in suspension was characterized via atomic force microscopy (AFM) (Nanosurf, Liestal, Switzerland, model EasyScan 2). For this test, the samples were prepared by coating the substrate with 0.01% LCNC suspension and dried at room temperature. The images obtained were analyzed with the software ImageJ 1.45 to determine the length and the thickness of the LCNC. Zeta potential was measured using a nanoparticle analyzer (NanoPartica SZ-100V2, Horiba, Japan).

#### 2.4. Composites Preparation

To make the composite PP/LCNC material, a Thermo Scientific twin-screw extruder was used with 8 heating zones with the following temperature profile: 170, 175, 180, 185, 190, 195 and 200 °C, respectively (Figure 2), with 1 bar of pressure at a spindle speed of 100 rpm, obtaining cylindrical profiles that were subsequently cut to obtain pellets of 32 × 12 mm. Mixtures with different percentages of LCNC as reinforcers were made in 100 g of polypropylene as the matrix (Table 1).

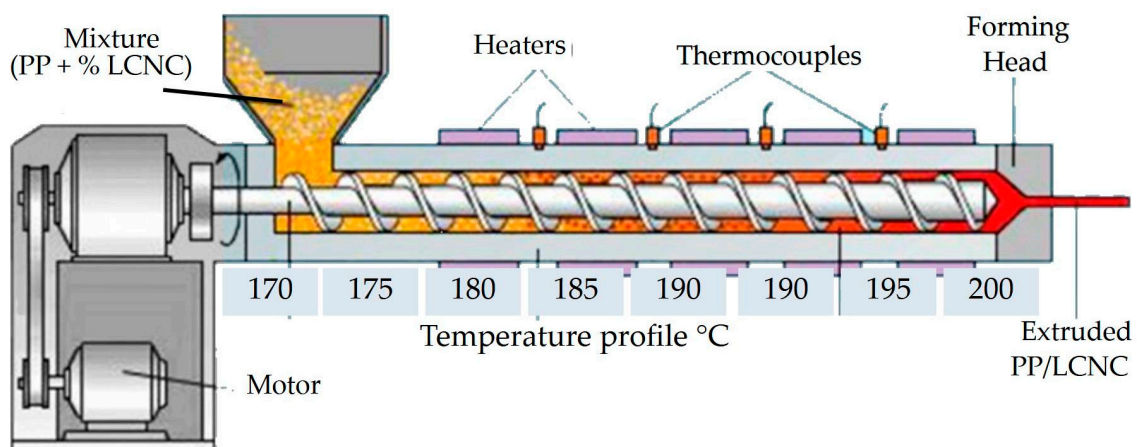


**Figure 2.** Graphic representation of the twin-screw extruder with its heating profile (8 zones).

**Table 1.** Mixtures of polypropylene with LCNC of corncob.

| Composite PP/LCNC's | % Polypropylene | % LCNC |
|---------------------|-----------------|--------|
| PP                  | 100             | 0      |
| PP/0.5%LCNC         | 99.5            | 0.5    |
| PP/1%LCNC           | 99              | 1      |
| PP/2%LCNC           | 98              | 2      |

Once the mixtures were made in the extruder and pelletized, the material was compression molded in a Susarrey model vulcanizing press using the following sequence: around 30 g of the mixtures was introduced into a mold with dimensions of 125 × 125 × 3 mm; the material was preheated for 3 min at 180 °C; then, it was thermo-compressed at 180 °C and 100 psig for 2 min; then, the bubbles in the material were released through decompression at 180 °C and 200 psig for 2 min; and finally, it is allowed to cool to 60 °C to obtain the plates. These plates were left to rest for 24 h to stabilize the environmental temperature and thus be able to carry out the tensile tests.

### 2.5. LCNC/PP Composites Characterization

The composite material LCNC/PP with polypropylene and lignocellulose nanocrystals (LCNCs), obtained by corncobs in the different percentages of mixtures, were characterized with different techniques and compared to a polypropylene material without LCNC. The following characterization techniques were carried out:

- Fourier-transform infrared spectroscopy (FTIR): FTIR analysis was carried out to determine the main functional groups on the LCNC/PP composite. The FTIR spectra were collected at a resolution of  $4\text{ cm}^{-1}$  in transmission mode ( $4000\text{--}400\text{ cm}^{-1}$ ) using a FTIR spectrophotometer Alpha, Bruker (Germany, Berlin). The spectra were plotted using Origin Pro 2019 software.
- Thermogravimetric analysis (TGA): The LCNC/PP composite was analyzed using a TGA-Q500 thermogravimetric analyzer (TA Instruments, New Castle, DE, USA) to study its thermal behavior. It was equipped with Universal Analysis 2000 software (version 4.5A, TA Instruments). Samples were heated from  $30\text{ }^{\circ}\text{C}$  to  $600\text{ }^{\circ}\text{C}$  at  $10\text{ }^{\circ}\text{C}/\text{min}$  under nitrogen. The spectra were plotted using Origin Pro 2019 software.
- Differential scanning calorimetry (DSC): To study the thermal transitions of pure PP and the PP/LCNC composite, the differential scanning calorimetry technique was used using the Perkin Elmer DSC equipment, Pyris DSC-6 (USA, TX, San Antonio), National University of Costa Rica, with a heating rate of  $20\text{ }^{\circ}\text{C}/\text{min}$  from room temperature to  $250\text{ }^{\circ}\text{C}$  in a nitrogen atmosphere. This energy difference was recorded as a spike on the DSC scan, indicating the temperature and energy of the transition.
- Mechanical properties: Tensile tests were measured on the Instron Model 3345 Universal Testing Machine (USA, IL, Glenview) with a 1 kN load cell. The standard used was ASTM D638 type IV specimen [31]. The crosshead speed was set at  $5\text{ mm}/\text{min}$  and room temperature. Reported values for the modulus, strength, and elongation at break were based on the average of at least five samples. Bending tests were carried out according to the ASTM D790 standard, which uses three points, two support and one on the top [32], for which the plates obtained after thermo-compression were taken and cut into rectangular specimens according to the standard and placed in the Instron Model 4411 Universal Testing Equipment, where they were vertically deformed at a constant temperature and constant speed with a minimum of 5 repetitions per trial.

## 3. Results and Discussion

### 3.1. Morphology of Corncob Fibers from Macro to Nano

Corncob is an agroindustrial waste product of corn shellings (Figure 3a). This is structurally divided into a medulla, woody ring and glume, which are morphologically organized in the form of fibers (Figure 3b). Its chemical composition is  $42.89 \pm 2.9\%$  cellulose,  $29.69 \pm 3.1\%$  hemicellulose,  $15.7 \pm 1.30\%$  lignin,  $9.94\%$  extractables and  $1.78 \pm 0.70\%$  ash [24]. These components are intimately intertwined with each other like any other lignocellulosic material. Accordingly, an organosolve pulping process was carried out on the corncob to extract the individualized cellulose fibers. With this, fibers with lengths of  $191 \pm 3.5$  microns and diameters of  $10 \pm 4.5$  microns were obtained (Figure 3c). It is important to highlight that these fibers were not bleached. For the unbleached organosolve cellulose fibers, hydrolysis was carried out, obtaining LCNCs. These structures are filaments that are in the order of nanometers. The acidic hydrolysis dissolved the non-crystalline regions of the fiber cellulose structure to obtain cellulose nanocrystals (Figure 3d). The AFM image shows that the LCNCs has a needle shape, confirming a successful extraction, and the average size was  $225.86 \pm 83.34\text{ nm}$  in length and  $36.92 \pm 12.36\text{ nm}$  in diameter. The zeta potential was  $-25 \pm 1.25$  in accordance with what was reported by Santos et al. in 2021 for unbleached CNC. This is a low value compared to other CNC studies, However, since the cellulose was unbleached, the presence of residual lignin influenced the surface interaction with the groups associated with sulfuric acid, causing a decrease in the ester groups of the sulfate ions ( $-\text{OSO}_3^-$ ) that are usually introduced into CNCs after hydrolysis with sulfuric acid [24].

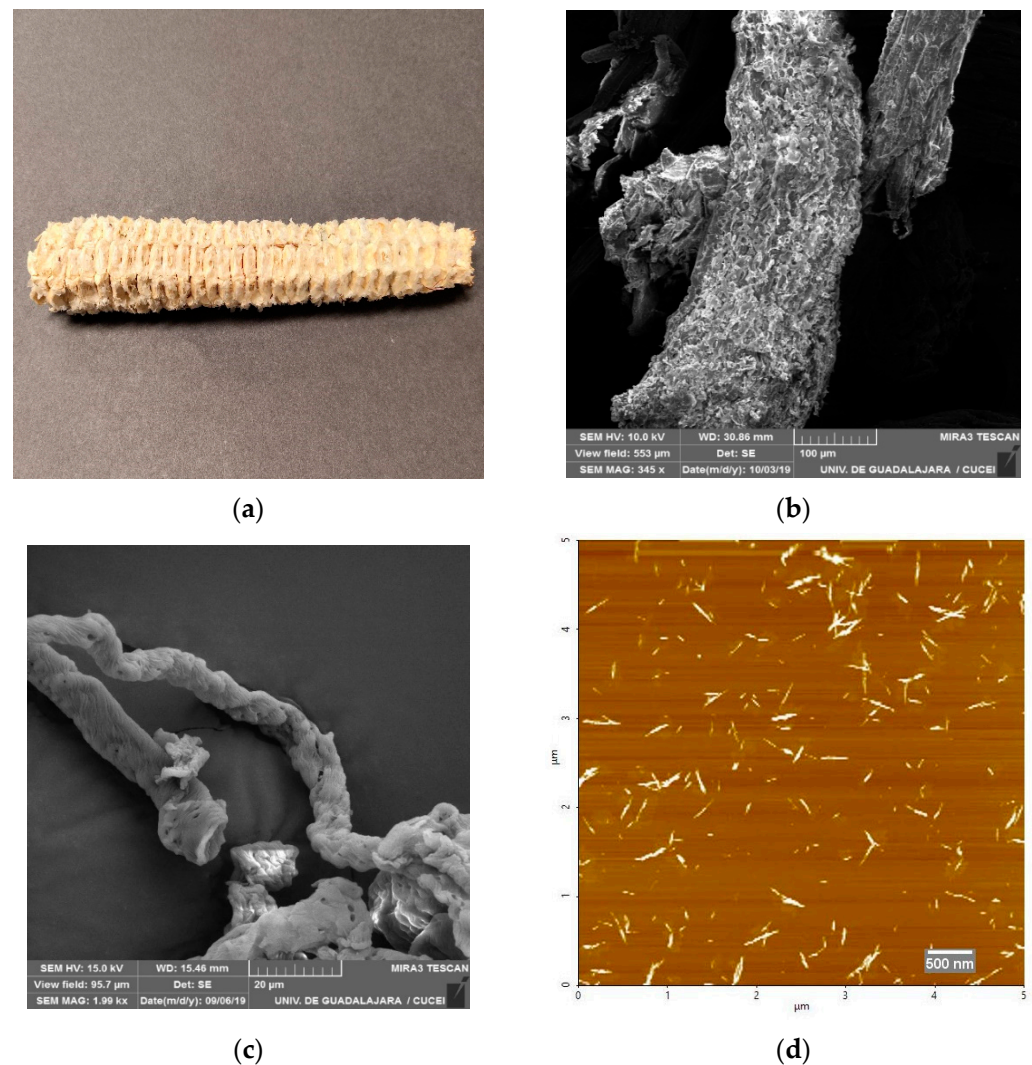


**Figure 3.** Images of different scales of the corncob fractionation: (a) digital photographs of corncob, (b) SEM images of fiber of corncobs, (c) Organosolv cellulose fibers from corncobs and (d) AFM images of LCNC from corncobs cellulose.

### 3.2. Infra-Red Spectroscopy with Fourier Transform (FT-IR)

The characterization of the corncob cellulose, LCNC and composite PP-LCNC obtained at different percentages (0.5, 1 and 2% LCNC) is analyzed (Figure 4). In Figure 4a, the characteristic signals of the cellulosic material are observed, such as  $3335\text{ cm}^{-1}$  corresponding to OH,  $2895\text{ cm}^{-1}$  corresponding to C-H bonds,  $1140\text{ cm}^{-1}$  and  $1030\text{ cm}^{-1}$  corresponding to C-C and C-O bonds and  $894\text{ cm}^{-1}$  corresponding to C-O-C. In the spectra of Figure 4b, the characteristic peaks of PP are clearly observed, which is the polymeric matrix with the highest proportion in composites. For PP the three groups of C-H bonds are observed at  $2900\text{ cm}^{-1}$ , C-C bonds at  $1350\text{--}1450\text{ cm}^{-1}$  and  $\text{-CH}_3$  bonds between  $1200$  and  $1000\text{ cm}^{-1}$ .

For the composites with LCNC, in addition to the PP peaks, the peaks are observed at  $3300\text{ cm}^{-1}$ , corresponding to the vibration of OH from the LCNC and aromatic benzene rings of lignin at  $1600\text{--}1500\text{ cm}^{-1}$  (Figure 4b) [28]. In previous works, it has been reported that lignin influences the interaction with groups associated with sulfuric acid, generating a partial functionalization of the hydroxyl groups on the surface with sulfate semi-esters, resulting in lignocellulose nanocrystals that have negative surface charges of the sulfate groups ( $\text{-OSO}_3$ ), and this is evidenced by the signal at  $1732\text{ cm}^{-1}$  in the LCNC FTIR (Figure 4a) [33–35]. However, this signal is not observed when the PP/LCNC composite

material is present since the LCNCs are embedded in the PP matrix, and the only lignin signal that can be observed is between  $1500$  and  $1600\text{ cm}^{-1}$ , which corresponds to the aromatic benzene rings of lignin, and this is more evident in PP/2%LCNC since it has the highest concentration of LCNCs. Therefore, it can be said that the interaction of residual lignin with PP occurs due to the surface charges of the sulfate groups, and this contributes to a better coupling with the polypropylene chains in the composite.

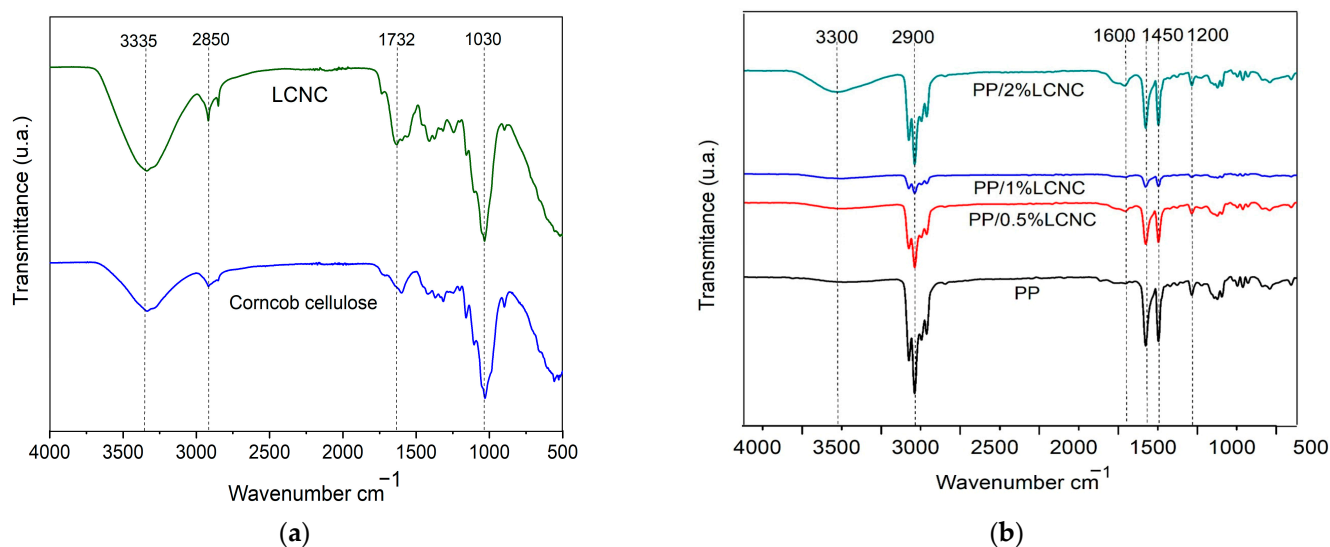


**Figure 4.** FT-IR spectra: (a) corncob al LCNC and (b) PP-LCNC composite with different LCNC contents.

### 3.3. Thermal Stability Analysis (TGA)

Figure 5a shows the thermogravimetric analysis of the PP-LCNC composites, and the composites and pure PP had a significant loss of mass up to  $300\text{ }^{\circ}\text{C}$ . After this temperature, both the PP and the PP-LCNC composites showed a sudden decrease in their weight loss (%), which suggests that the composite material degrades above this temperature ( $300\text{ }^{\circ}\text{C}$ ). Finally, it was observed that at  $500\text{ }^{\circ}\text{C}$ , the material had been completely carbonized due to the constant weight that it kept after this temperature. Figure 5b shows the differential thermogravimetric analysis (DTG), where it can be seen that the maximum thermal decomposition point is observed at  $483\text{ }^{\circ}\text{C}$  for pure PP. This was different to the composites with LCNCs. From this graph, it can be seen that for PP/0.5%LCNC, it was  $488\text{ }^{\circ}\text{C}$ , for PP/1%LCNC, it was  $490\text{ }^{\circ}\text{C}$  and for PP/2%LCNC, it was  $486\text{ }^{\circ}\text{C}$ . The residual lignin present in LCNCs has a role in the thermal degradation of PP/LCNC composites, since lignin is full of aromatic rings with several branches that make it difficult to degrade between  $100$  and  $900\text{ }^{\circ}\text{C}$  [23,36]. This chemical composition of residual lignin causes the degradation temperature in the PP/LCNC composite material to increase. This indicates that by adding LCNCs to the PP matrix, the maximum degradation point increases due to the presence of residual lignin in the cellulose nanocrystals, favoring its thermal resistance, and this implies that the composite material can have more possibilities of use.

Table 2 summarizes the most important values of the TGA thermograms for all the samples analyzed, where it was highlighted that the variations in degradation temperatures with 50% mass loss were higher when using LCNCs between  $482$  and  $475\text{ }^{\circ}\text{C}$  in comparison with pure polypropylene, which was  $473\text{ }^{\circ}\text{C}$ . This may be caused by the different matrix–reinforcement interactions and the dispersion of LNCCs in the matrix at different concentrations [37]. Another important thing is that, in all the samples, a percentage of the residual mass at  $600\text{ }^{\circ}\text{C}$  of approximately  $11\% \pm 1$  was obtained; this may be due to the presence of some inorganic-type additives present in the PP matrix of the composite [37] and the presence of residual lignin since it is degraded at higher temperatures [23].

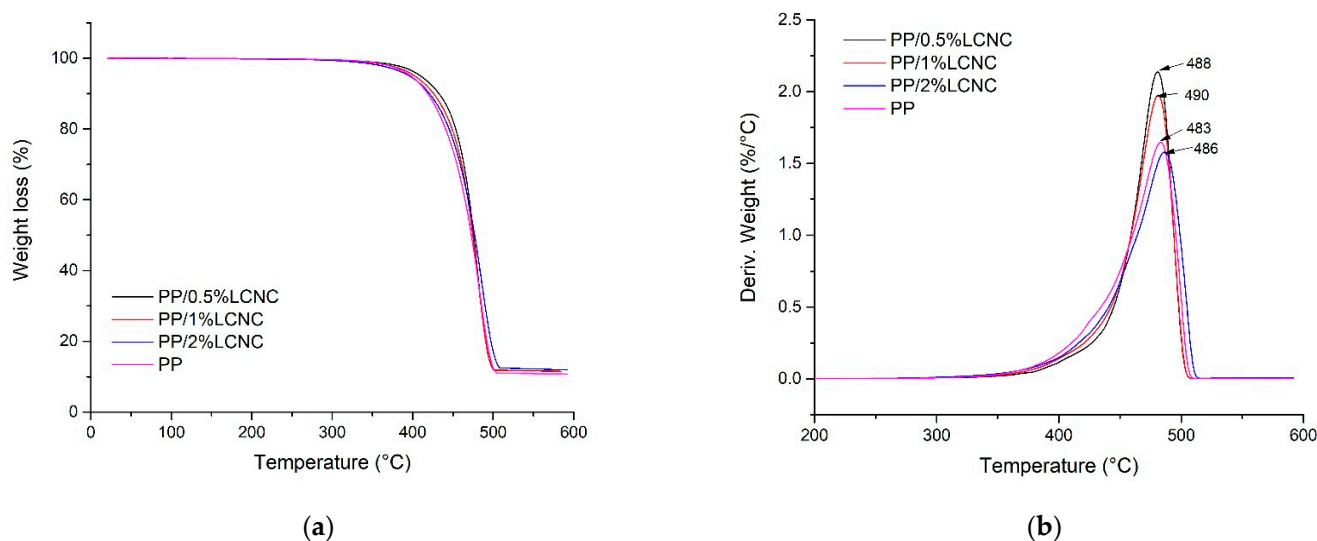


**Figure 5.** TGA analysis: (a) TGA thermograms of PP/LCNC composites and (b) DTGA curves of PP/LCNC composites.

**Table 2.** Thermal properties of the samples obtained from the PP/CNC composites.

| Composite   | Initial Degradation Temperature (°C) | Final Degradation Temperature (°C) | Degradation Temperature with 50% Mass Loss (°C) | % Residual Mass at 600 °C | DTG T Max (°C) |
|-------------|--------------------------------------|------------------------------------|---|---------------------------|----------------|
| PP          | 406                                  | 497                                | 473   | 10.81                     | 483            |
| PP/0.5%LCNC | 443                                  | 500                                | 482   | 11.53                     | 488            |
| PP/1%LCNC   | 438                                  | 502                                | 483   | 11.58                     | 490            |
| PP/2%LCNC   | 424                                  | 500                                | 475   | 11.92                     | 486            |

### 3.4. Analysis of Thermal Transitions (DSC)

Differential scanning calorimetry analysis was also performed on the materials composed of polypropylene and cellulose nanocrystals. Figure 6 shows the DSC thermograms obtained, where the melting or boiling points were seen as a downward peak (endothermic) since they absorb energy.

Figure 6 shows the DSC graphs for PP and PP/LCNC composites, from which it is possible to see in all samples two endothermic peaks. The main peak is at 163.65 °C for pure PP, and the peak of the composites oscillate between 164.94 °C and 164.97 °C, which is associated with the melting point of PP reported by other authors [23,38,39]. The second peak is not as pronounced (126 °C) and can be associated with the fact that the recycled PP has fractions of another polymer [38]. Table 3 shows the endothermic peak, the crystallinity and the enthalpies of melting of the DSC thermograms obtained for PP and PP/LCNC composites. The crystallinity is low for recycling PP (53%) and decreases when adding 0.5 and 2% of LCNCs (49.47% and 50.7%, respectively). This result is in accordance with the reported ones by other author, for composite material with PP and LCNC/unbleached cellulose. The authors attribute this effect to the fact that LCNCs are not distributed well and that LNCCs added to the molecular chains are less likely to diffuse towards the nucleus of the crystal, and this can reduce the rate of crystal growth, which is reflected in the decrease in crystallinity [23]. In spite of this, the data indicated that the percentage of 1% of LCNC content increased by 3% the crystalline and melting enthalpy values of the composites. In this case, it could be that 2% of LCNCs are distributed better [40].

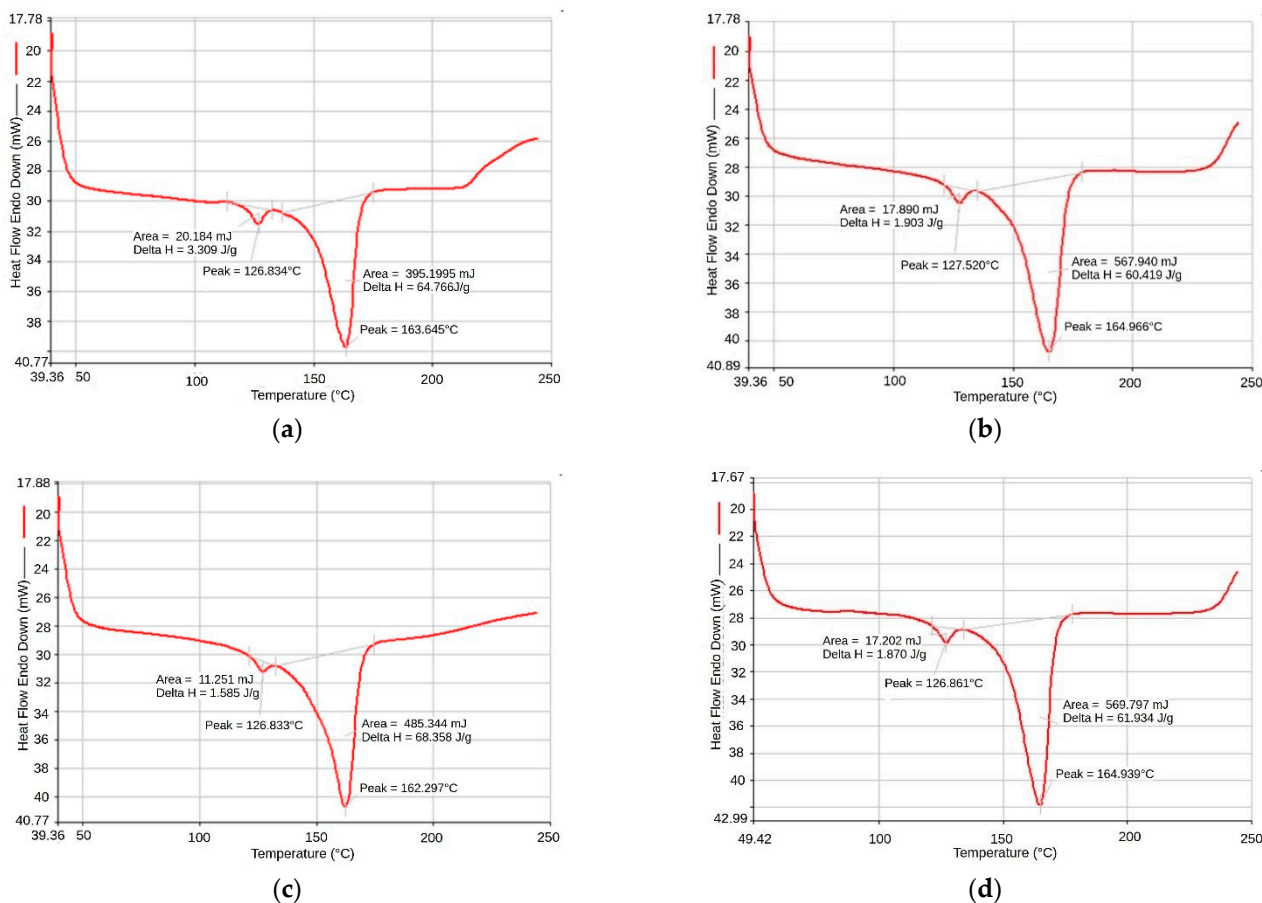


Figure 6. DSC: (a) PP, (b) PP/0.5%LCNC, (c) PP/1%LCNC and (d) PP/2%LCNC.

Table 3. DSC results of the composites obtained from the PP/LCNC blends.

| Composite   | Enthalpy $\Delta H_f$ (J/g) | Crystallinity (%) | First Endothermic Peak (°C) | Second Endothermic Peak (°C) |
|-------------|-----------------------------|-------------------|-----------------------------|------------------------------|
| PP          | 64.786                      | 53.03             | 126.834                     | 163.645                      |
| PP/0.5%LCNC | 60.419                      | 49.47             | 127.520                     | 164.966                      |
| PP/1%LCNC   | 68.358                      | 55.97             | 126.833                     | 162.297                      |
| PP/2%LCNC   | 61.934                      | 50.71             | 126.861                     | 164.939                      |

### 3.5. Tensile Tests

Figure 7 shows the Young’s modulus due to traction of the PP and PP/LCNC composites, with 0.5, 1 and 2% LCNC, respectively. It can be observed that the Young’s modulus increases as the percentage of the LCNC increases. In a previous study [41], it was shown that the Young’s modulus of PP/CNC mixes increased with a higher CNC content. In addition, the values (784 MPa) for the Young’s modulus of pure PP are lower than those of the composites; this is due to the greater rigidity of their chains, as previously identified with DSC thermograms [40]. On the other hand, the residual lignin of the LCNC, as previously seen in the IRs obtained, causes greater rigidity in the composite. For example, in composites with 2% LCNC, the composite has an increase in Young’s modulus compared to composites containing 0.5% LCNC from 793.23 MPa to 838.15 MPa; these results are similar to those obtained in the work of Gray 2018 [40].

The tensile strength was evaluated in PP and PP/LCNC, as shown in Figure 7b. In this graph, it can be seen that the tensile strength acts in a similar way to Young’s modulus since, in the PP/LCNC composites, there is a greater magnitude in the tensile strength values compared to pure PP. Increasing the concentration of LCNC (1 and 2%) increases the

traction for each compound. In the case of samples with 0.5% LCNC, the tensile strength (Figure 7b) is lower than PP because the LCNCs were not distributed well and could have been loaded on the side where the stretching was carried out, resulting in a faster rupture. However, the Young’s modulus graph (Figure 7a) shows the increase in the modulus; these data indicate the rigidity of the material since it is the slope at which it has an elastic behavior until it reaches the rupture, while the tensile stress only indicates the stress against elongation and the fracture time [40].

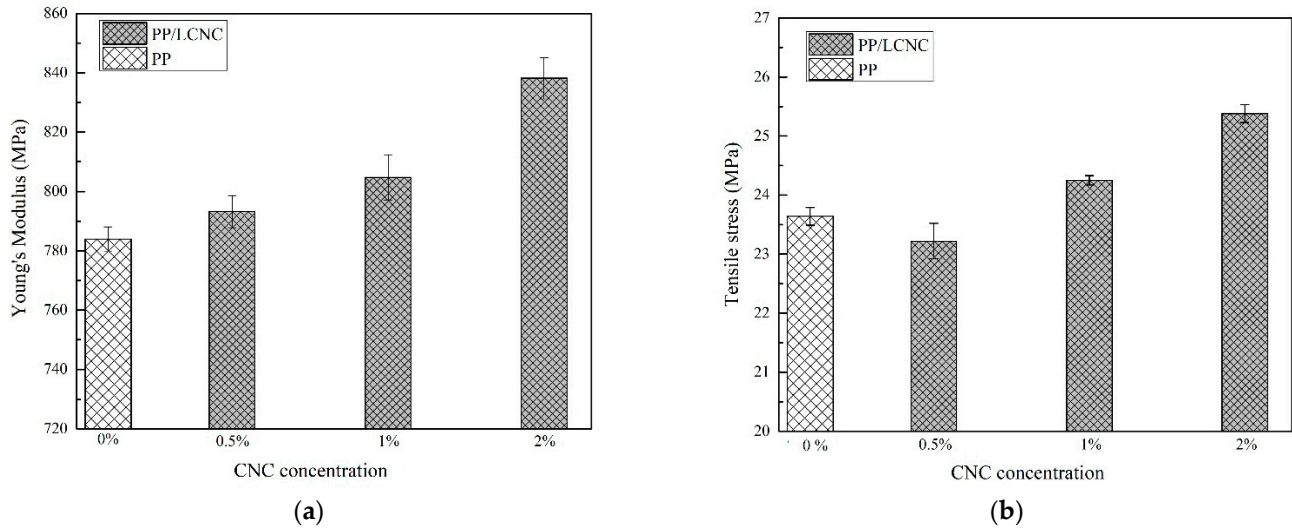


Figure 7. Tensile tests: (a) Young’s modulus due to traction of PP/LCNC composites and (b) tensile strength of PP/LCNC composites.

### 3.6. Bending Tests

Regarding bending, Figure 8a shows the results of the flexural modulus of the PP/LCNC composites, where it can be analyzed that, as in tension, the Young’s modulus, due to traction, increases with increasing the amount of LCNCs. A significant increase in the flexural modulus of 36% is observed for the composite with 2% LCNC with respect to net PP. This may be due to the fact that both in tension and in bending, more LCNCs have a better interaction and accommodation in the polymeric matrix (PP) [38] due to the residual lignin present in the LCNCs, which acts as a natural glue between the LCNCs and the polymeric matrix (PP) [33].

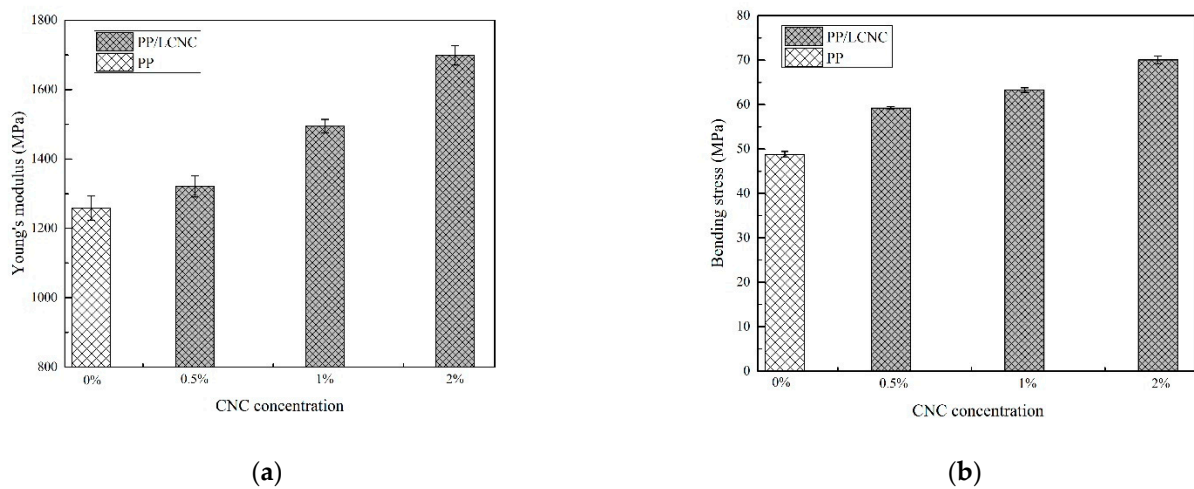


Figure 8. Bending tests: (a) Young’s modulus due to traction of PP/LCNC composites, (b) bending strength of PP/LCNC composites.

Regarding the bending strength (Figure 8), it follows the same behavior as the tensile strength, since the flexural strength increases by 43% for the composite with 2% CNTC with respect to net PP. It can be noted that the PP/LCNC composites have higher bending strengths than PP; this is due to the greater amount of residual lignin in the LCNC and is in accordance with previous studies, where it is mentioned that lignin acts as a natural glue that makes the structure of the chains more rigid, and the presence of residual lignin [25] can be verified in the IRs of the composites obtained in this work.

#### 4. Conclusions

In this research, it was possible to prepare a recycled PP composite material with different concentrations of CNCs with residual lignin (LCNC) from unbleached corncob cellulose. These materials were evaluated for their mechanical and thermal properties. According to the results obtained, the following conclusions are highlighted:

- The presence of residual lignin in the unbleached cellulose of corncob generates functionalization on the surface of the LCNCs, one by residual lignin and the other by the ester groups of the sulfate ions ( $-\text{OSO}_3^-$ ) introduced after hydrolysis with sulfuric acid due to the esterification between the surface hydroxyls of unbleached cellulose and sulfuric acid.
- This functionalization by residual lignin and the ester groups improved the interaction between LCNCs and polypropylene, improving the thermal and mechanical properties in the composite material.
- In general, all concentrations of LCNC in composite material showed to be thermally stable for processing, but it is noteworthy that the melting enthalpies was increased by adding 2% of LCNC compared to pure PP.
- Based on the results obtained from the mechanical tests, it was possible to demonstrate that the composite is resistant to traction and bending compared to pure recycled PP. Young's modulus and bending strengths increase as the percentage of LCNC increases, and the tensile strength acts similarly to Young's modulus.
- The interaction between LCNC and PP is good, and there is an accommodation of the filler in the polymer matrix, which implies better mechanical properties.

**Author Contributions:** Conceptualization, M.A.E.-Á. and B.S.-R.; methodology, E.M.S.-V. and M.E.-A.; formal analysis, R.G.-N., M.E.-A. and B.S.-R.; writing—original draft preparation, E.M.S.-V.; writing—review and editing, R.G.-N., B.S.-R. and M.A.E.-Á. All authors have read and agreed to the published version of the manuscript.

**Funding:** The funding was received from Universidad Nacional de Costa Rica.

**Institutional Review Board Statement:** Not applicable.

**Informed Consent Statement:** Not applicable.

**Data Availability Statement:** Data are contained within the article.

**Acknowledgments:** The authors would like to thank the nanotechnology engineering students and social service providers at the University of Guadalajara Campus Tonalá for their laboratory support.

**Conflicts of Interest:** The authors declare no conflicts of interest.

#### References

1. Tian, H.; Wu, L.; Qin, H.; Li, X.; Zhao, X.; Zhao, W.; Xue, F.; Zhao, S.; Li, L.; Zeng, W. Composite materials combined with stem cells promote kidney repair and regeneration. *Compos. Part B Eng.* **2024**, *275*, 111278. [[CrossRef](#)]
2. Yadav, R.; Singh, M.; Shekhawat, D.; Lee, S.-Y.; Park, S.-J. The role of fillers to enhance the mechanical, thermal, and wear characteristics of polymer composite materials: A review. *Compos. Part A Appl. Sci. Manuf.* **2023**, *175*, 107775. [[CrossRef](#)]
3. Nahar, S.; Khan, R.A.; Dey, K.; Sarker, B.; Das, A.K.; Ghoshal, S. Comparative studies of mechanical and interfacial properties between jute and bamboo fiber-reinforced polypropylene-based composites. *J. Thermoplast. Compos. Mater.* **2012**, *25*, 15–32. [[CrossRef](#)]

4. Varshney, D.; Debnath, K.; Singh, I. Mechanical characterization of polypropylene (PP) and polyethylene (PE) based natural fiber reinforced composites. *Int. J. Surf. Eng. Mater. Technol.* **2014**, *4*, 16–23.
5. Mohammadi, M.; Taban, E.; Tan, W.H.; Che Din, N.B.; Putra, A.; Berardi, U. Recent progress in natural fiber reinforced composite as sound absorber material. *J. Build. Eng.* **2024**, *84*, 108514. [[CrossRef](#)]
6. Zhiltsova, T.; Campos, J.; Costa, A.; Oliveira, M.S.A. Sustainable Polypropylene-Based Composites with Agro-Waste Fillers: Thermal, Morphological, Mechanical Properties and Dimensional Stability. *Materials* **2024**, *17*, 696. [[CrossRef](#)]
7. Song, D.; Wang, B.; Tao, W.; Wang, X.; Zhang, W.; Dai, M.; Li, J.; Zhou, Z. Synergistic reinforcement mechanism of basalt fiber/cellulose nanocrystals/polypropylene composites. *Nanotechnol. Rev.* **2022**, *11*, 3020–3030. [[CrossRef](#)]
8. Wang, X.; Wang, P.; Liu, S.; Crouse, J.; Gardner, D.J.; Via, B.; Gallagher, T.; Elder, T.; Peng, Y. Material properties of spray-dried cellulose nanocrystal reinforced homopolymer polypropylene composites. *Polym. Compos.* **2023**. [[CrossRef](#)]
9. Teruel, R.; Alcalá, N.; Crespo, C.; Laspalas, M. Machine learning model and input batch management tool for the composition of new recycled polypropylene plastic material with reduced variability in target properties. *J. Clean. Prod.* **2024**, *435*, 140390. [[CrossRef](#)]
10. Prado, K.S.; Strangl, M.; Pereira, S.R.; Tiboni, A.R.; Ortner, E.; Spinacé, M.A.S.; Buettner, A. Odor characterization of post-consumer and recycled automotive polypropylene by different sensory evaluation methods and instrumental analysis. *Waste Manag.* **2020**, *115*, 36–46. [[CrossRef](#)]
11. Khoshkava, V.; Kamal, M.R. Effect of cellulose nanocrystals (CNC) particle morphology on dispersion and rheological and mechanical properties of polypropylene/CNC nanocomposites. *ACS Appl. Mater. Interfaces* **2014**, *6*, 8146–8157. [[CrossRef](#)]
12. Bagheriasl, D.; Carreau, P.J.; Dubois, C.; Riedl, B. Effect of cellulose nanocrystals (CNCs) on crystallinity, mechanical and rheological properties of polypropylene/CNCs nanocomposites. *AIP Conf. Proc.* **2015**, *1664*, 070010. [[CrossRef](#)]
13. Sojoudiasli, H.; Heuzey, M.-C.; Carreau, P.J. Mechanical and morphological properties of cellulose nanocrystal-polypropylene composites. *Polym. Compos.* **2018**, *39*, 3605–3617. [[CrossRef](#)]
14. Agarwal, J.; Mohanty, S.; Nayak, S.K. Valorization of pineapple peel waste and sisal fiber: Study of cellulose nanocrystals on polypropylene nanocomposites. *J. Appl. Polym. Sci.* **2020**, *137*, 49291. [[CrossRef](#)]
15. Gwon, J.-G.; Cho, H.-J.; Lee, D.; Choi, D.-H.; Lee, S.; Wu, Q.; Lee, S.-Y. Physicochemical and mechanical properties of polypropylene-cellulose nanocrystal nanocomposites: Effects of manufacturing process and chemical grafting. *BioResources* **2018**, *13*, 1619–1636. [[CrossRef](#)]
16. Huang, J.; Xu, C.; Wu, D.; Lv, Q. Transcrystallization of polypropylene in the presence of polyester/cellulose nanocrystal composite fibers. *Carbohydr. Polym.* **2017**, *167*, 105–114. [[CrossRef](#)] [[PubMed](#)]
17. Bagheriasl, D.; Carreau, P.J.; Dubois, C.; Riedl, B. Properties of polypropylene and polypropylene/poly(ethylene-co-vinyl alcohol) blend/CNC nanocomposites. *Compos. Sci. Technol.* **2015**, *117*, 357–363. [[CrossRef](#)]
18. Ghabezi, P.; Farahani, M.; Hosseini Fakhr, M. Experimental investigation of nano-alumina effect on the filling time in VARTM process. *J. Fundam. Appl. Sci.* **2016**, *8*, 925. [[CrossRef](#)]
19. Ghabezi, P.; Farahani, M.; Hosseini Fakhr, M.; Abroshan, H. Investigation of Mechanical Behavior of Alfa and Gamma Nano-Alumina/Epoxy Composite Made By Vartm. *Int. J. Adv. Biotechnol. Res.* **2016**, *7*, 731–736.
20. Görbe, Á.; Varga, L.J.; Bárány, T. Development of nanoparticle-filled polypropylene-based single polymer composite foams. *Heliyon* **2023**, *9*, e19638. [[CrossRef](#)]
21. Shojaeiarani, J.; Bajwa, D.S.; Chanda, S. Cellulose nanocrystal based composites: A review. *Compos. Part C Open Access* **2021**, *5*, 100164. [[CrossRef](#)]
22. Trache, D.; Thakur, V.K.; Boukherroub, R. Cellulose Nanocrystals/Graphene Hybrids—A Promising New Class of Materials for Advanced Applications. *Nanomaterials* **2020**, *10*, 1523. [[CrossRef](#)]
23. Sabaruddin, F.A.; Paridah, M.T.; Sapuan, S.M.; Ilyas, R.A.; Lee, S.H.; Abdan, K.; Mazlan, N.; Roseley, A.S.; Abdul Khalil, H.P.S. The Effects of Unbleached and Bleached Nanocellulose on the Thermal and Flammability of Polypropylene-Reinforced Kenaf Core Hybrid Polymer Bionanocomposites. *Polymers* **2020**, *13*, 116. [[CrossRef](#)] [[PubMed](#)]
24. Santos Ventura, E.M.; Alfredo, E.Á.M.; Gutiérrez Becerra, A.; Sulbarán-Rangel, B. Unbleached cellulose from waste corn cob for isolation of cellulose nanocrystals. *Emerg. Mater. Res.* **2020**, *9*, 1258–1265. [[CrossRef](#)]
25. Peng, Y.; Nair, S.S.; Chen, H.; Yan, N.; Cao, J. Effects of Lignin Content on Mechanical and Thermal Properties of Polypropylene Composites Reinforced with Micro Particles of Spray Dried Cellulose Nanofibrils. *ACS Sustain. Chem. Eng.* **2018**, *6*, 11078–11086. [[CrossRef](#)]
26. *ISO 1133; Plastics—Determination of Melt Flow Rate (MFR) and Melt Volume Flow Rate (MVR) of Thermoplastics*. ISO: Geneva, Switzerland, 2012.
27. *ISO 1183; Plastics—Methods for Determining the Density of Non-Cellular Plastics—Part 1: Immersion Method, Liquid Pycnometer Method and Titration Method*. ISO: Geneva, Switzerland, 2019.
28. Gutiérrez-Hernández, J.M.; Escalante, A.; Murillo-Vázquez, R.N.; Delgado, E.; González, F.J.; Toríz, G. Use of Agave tequilana-lignin and zinc oxide nanoparticles for skin photoprotection. *J. Photochem. Photobiol. B Biol.* **2016**, *163*, 156–161. [[CrossRef](#)]
29. Hernández, J.A.; Romero, V.H.; Escalante, A.; Toríz, G.; Rojas, O.J.; Sulbarán, B.C. Agave tequilana bagasse as source of cellulose nanocrystals via organosolv treatment. *BioResources* **2018**, *13*, 3603–3614. [[CrossRef](#)]
30. Cranston, E.D.; Gray, D.G. Formation of cellulose-based electrostatic layer-by-layer films in a magnetic field. *Sci. Technol. Adv. Mater.* **2006**, *7*, 319. [[CrossRef](#)]

31. ASTM D638-22; Standard Test Method for Tensile Properties of Plastics. ASTM: West Conshohocken, PA, USA, 2022.
32. ASTM D790-17; Standard Test Methods for Flexural Properties of Unreinforced and Reinforced Plastics and Electrical Insulating Materials. ASTM: West Conshohocken, PA, USA, 2017.
33. Lin, N.; Dufresne, A. Surface chemistry, morphological analysis and properties of cellulose nanocrystals with gradiented sulfation degrees. *Nanoscale* **2014**, *6*, 5384–5393. [[CrossRef](#)] [[PubMed](#)]
34. Bilatto, S.; Marconcini, J.M.; Mattoso, L.H.C.; Farinas, C.S. Lignocellulose nanocrystals from sugarcane straw. *Ind. Crops Prod.* **2020**, *157*, 112938. [[CrossRef](#)]
35. Liang, F.; Song, Y.; Huang, C.; Zhang, J.; Chen, B. Preparation and performance evaluation of a lignin-based solid acid from acid hydrolysis lignin. *Catal. Commun.* **2013**, *40*, 93–97. [[CrossRef](#)]
36. Yang, H.; Yan, R.; Chen, H.; Lee, D.H.; Zheng, C. Characteristics of hemicellulose, cellulose and lignin pyrolysis. *Fuel* **2007**, *86*, 1781–1788. [[CrossRef](#)]
37. Tsiptsias, C.; Leontiadis, K.; Tzimpilis, E.; Tsivintzelis, I. Polypropylene nanocomposite fibers: A review of current trends and new developments. *J. Plast. Film Sheeting* **2021**, *37*, 283–311. [[CrossRef](#)]
38. Monti, M.; Scrivani, M.T.; Gianotti, V. Effect of SEBS and OBC on the Impact Strength of Recycled Polypropylene/Talc Composites. *Recycling* **2020**, *5*, 9. [[CrossRef](#)]
39. Majewsky, M.; Bitter, H.; Eiche, E.; Horn, H. Determination of microplastic polyethylene (PE) and polypropylene (PP) in environmental samples using thermal analysis (TGA-DSC). *Sci. Total Environ.* **2016**, *568*, 507–511. [[CrossRef](#)] [[PubMed](#)]
40. Gray, N.; Hamzeh, Y.; Kaboorani, A.; Abdulkhani, A. Influence of cellulose nanocrystal on strength and properties of low density polyethylene and thermoplastic starch composites. *Ind. Crops Prod.* **2018**, *115*, 298–305. [[CrossRef](#)]
41. Habibi, Y.; Lucia, L.A.; Rojas, O.J. Cellulose nanocrystals: Chemistry, self-assembly, and applications. *Chem. Rev.* **2010**, *110*, 3479–3500. [[CrossRef](#)]

**Disclaimer/Publisher’s Note:** The statements, opinions and data contained in all publications are solely those of the individual author(s) and contributor(s) and not of MDPI and/or the editor(s). MDPI and/or the editor(s) disclaim responsibility for any injury to people or property resulting from any ideas, methods, instructions or products referred to in the content.